Nanoscale

Accepted Manuscript

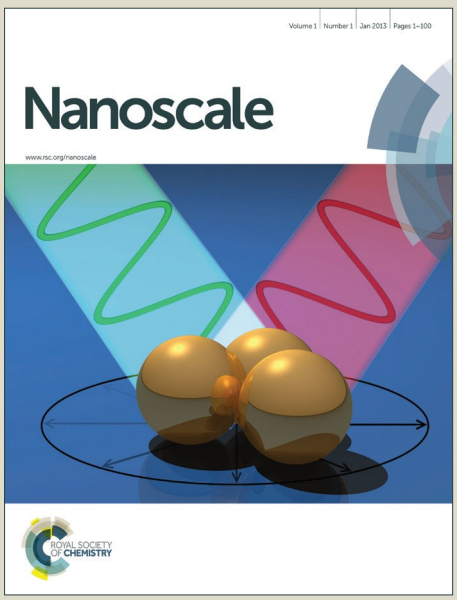

This is an *Accepted Manuscript*, which has been through the Royal Society of Chemistry peer review process and has been accepted for publication.

Accepted Manuscripts are published online shortly after acceptance, before technical editing, formatting and proof reading. Using this free service, authors can make their results available to the community, in citable form, before we publish the edited article. We will replace this *Accepted Manuscript* with the edited and formatted *Advance Article* as soon as it is available.

You can find more information about *Accepted Manuscripts* in the Information for Authors.

Please note that technical editing may introduce minor changes to the text and/or graphics, which may alter content. The journal's standard Terms & Conditions and the Ethical guidelines still apply. In no event shall the Royal Society of Chemistry be held responsible for any errors or omissions in this *Accepted Manuscript* or any consequences arising from the use of any information it contains.

ROYAL SOCIETY OF CHEMISTRY

www.rsc.org/nanoscale

Nanoscale Stabilization of Zintl Compounds: 1D Ionic Li-P Double Helix Confined Inside a Carbon Nanotube

Alexander S. Ivanov,*[‡] Tapas Kar and Alexander I. Boldyrev

Department of Chemistry and Biochemistry, Utah State University, 0300 Old Main Hill, Logan, Utah 84322, United States

Corresponding Author:

*Email: ivanova@ornl.gov

Phone: (865) 5761753

Fax: (865) 5767956

Present Address:

[‡]Oak Ridge National Laboratory, Chemical Sciences Division, 1 Bethel Valley Rd., Oak Ridge, Tennessee, 37831-6119, United States

This submission was written by the author acting in his own independent capacity and not on behalf of UT-Battelle, LLC, or its affiliates or successors

Nanoscale Accepted Manuscript

ABSTRACT

One-dimensional (1D) ionic nanowires are extremely rare materials due to the difficulty in stabilizing 1D chains of ions under ambient conditions. We demonstrate here a theoretical prediction of a novel hybrid material, nanotube encapsulated 1D ionic lithium monophosphide (LiP) chain featuring unique double-helix structure, which is very unusual in inorganic chemistry. This nanocomposite has been investigated with density functional theory, including molecular dynamics simulations and electronic structure calculations. We find that formation of the LiP double-helical nanowire is facilitated by the strong interaction between LiP and CNTs resulting in a charge transfer. This work suggests that nanostructured confinement may be used to stabilize other polyphosphide 1D chains thus opening new ways to study the chemistry of Zintl compounds at the nanoscale.

1. INTRODUCTION

Materials with reduced dimensionality have recently received a lot of attention owing to not only their unique and appealing structures, but also their intriguing and useful properties that are very different from those of their bulk counterparts. Low-dimensional systems can exhibit extraordinary mechanical, electronic, thermal, optical, and chemical properties, which represent a potential interest for their use in a wide range of nanotechnology. For example, two-dimensional (2D) materials such as graphene, transition metal dichalcogenides, and phosphorene have already shown their importance for future nanodevices by having remarkable optical, electronic, and transport properties.[1-6] One can apply a further dimensional constraint on 2D

Nanoscale Accepted Manuscript

systems in order to get one-dimensional (1D) materials, which may presumably show a kaleidoscope of even more intriguing phenomena.

A variety of 1D systems have been synthesized, including semiconductor nanowires,[7-11] nanobelts,[12-14] coaxial nanocables,[15,16] gold,[17,18] silver,[18,19] and carbon monoatomic chains.[20-22] In addition, 1D SiC,[23] Pb_2O,[24] GeTe[25] and other materials[26] with their unique helical topologies have successfully been prepared. Although double-helical nanostructures are common in self-assembled organic systems[27,28] and biology,[29,30] similar nanostructures are very rare in 1D inorganic materials[31] and are represented by just a few examples.[32-35] In 2012 we reported the first theoretical evidence of the existence of the smallest inorganic LiP chiral clusters with peculiar double-helix morphologies.[36] For Li_7P_7-Li_9P_9 stoichiometries the global minimum structure consists of two strands, one composed of lithium cations and one composed of phosphorus anions, which run in opposite directions to each other and are therefore antiparallel. Subsequent periodic solid-state calculations also confirmed the stability of the infinite double-helical chain of Li and P ions. Later, using chemical bonding analysis, it was shown that the simple inorganic double helices represent a bonding picture very similar to that of nature's double-helical DNA.[37] Moreover, the unique self-healing property, which is mainly attributed to H-bonded and "smart" materials,[38,39] was observed in the inorganic LiP nanowires.[37] However, despite a huge fundamental interest and the predicted attractive properties for future nanotechnology applications, the LiP 1D inorganic double helices have not yet been synthesized. A possible reason preventing their fabrication is that a free-standing chain of Li and P ions would be unstable at ambient conditions because the number of coordinating counter-ions in this 1D structure is very small. To overcome this problem carbon nanotubes (CNTs) have vigorously been employed as templates for synthesis of nanostructured materials,[40] including 1D KI,[41] AgI,[42]

Nanoscale Accepted Manuscript

CsI,[43] and S[44] nanowires. The confined crystals are stabilized and constrained in cross-section by the van der Waals surface of the encapsulating CNTs. These next generation materials can be synthesized on a bulk scale and can potentially form the basis of single electron transistors,[45] logic circuits,[46] and memory elements.[47]

Here we report a theoretical prediction of the nanotube encapsulated 1D ionic LiP nanowires in which the cations and anions arranged to form the double-helical structure. Our density functional theory (DFT) computations demonstrate that this LiP double helix, confined inside a single-walled carbon nanotube (LiP@SWCNT), has excellent stability and thus has a potential for experimental realization. Although some advances have been achieved for CNT encapsulated 1D inorganic materials with covalently bonded selenium[48] and iodine double helices,[49] there were no reports on the CNT confined Zintl phase phosphide compounds and 1D ionic crystals with a double-helix structure that consists of both cations and anions.

2. RESULTS AND DISCUSSION

Lithium monophosphide (LiP) is an electron-balanced semiconductor in the bulk three-dimensional (3D) structure under ambient conditions and represents a monoclinic solid with $P2_1/c$ space group.[50] The phosphorus atoms form singly bonded infinite spiral chains in the LiP structure, whereas the lithium atoms are in positions defined approximately by a spiral coaxial with the phosphorus chains, but with a larger radius (Fig. 1a). From this monoclinic phase it is possible to hypothetically extract a 1D LiP chain exhibiting a double-helical configuration (Fig. 1b).

Nanoscale Accepted Manuscript

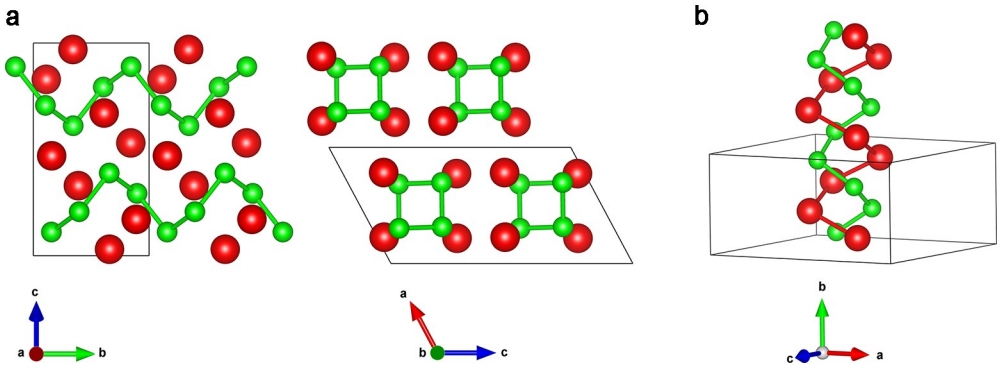

Fig. 1 (a) Crystal structure of $P2_1/c$ symmetric LiP bulk phase along different crystallographic directions. (b) 1D LiP double-helix chain geometry. Color scheme: Li, red; P, green.

This 1D system has been predicted by the previous DFT calculations and it is 9.69 kcal mol^{-1} higher in energy than the $P2_1/c$ symmetric LiP bulk phase.[36] We have probed three zigzag single-walled carbon nanotubes (SWCNTs) with different diameters *d* (SWCNT(10,0), *d* = 0.79 nm; SWCNT(12,0), *d* = 0.79 nm; and SWCNT(15,0), *d* = 1.19 nm; where (10,0), (12,0), and (15,0) denote chiral indices specifying the way the graphene sheet is wrapped to form the corresponding SWCNTs) as nanoscale matrices to host 1D ionic LiP double-helical chain. Our choice was motivated by the following factors: (i) single-walled carbon nanotubes (SWNTs) can be experimentally produced within a strictly limited diameter range. (ii) Their internal van der Waals surface controls the alignment of atoms and also the crystal growth of materials very precisely. (iii) The size of the inner surfaces of the SWNTs should correspond to the external dimensions of the encapsulated material, but at the same time smaller than that for two adjacent LiP rows in order to make the formation of 1D chains of Li and P ions possible. Calculations performed using SWCNTs of smaller diameter resulted in Li ions attaching to the inner nanotube wall that consequently broke the LiP double-helical geometry. Fig. 2 shows the LiP chains

Nanoscale Accepted Manuscript

confined inside the SWCNTs of different sizes. Each model contains four periodic repetitions of LiP.

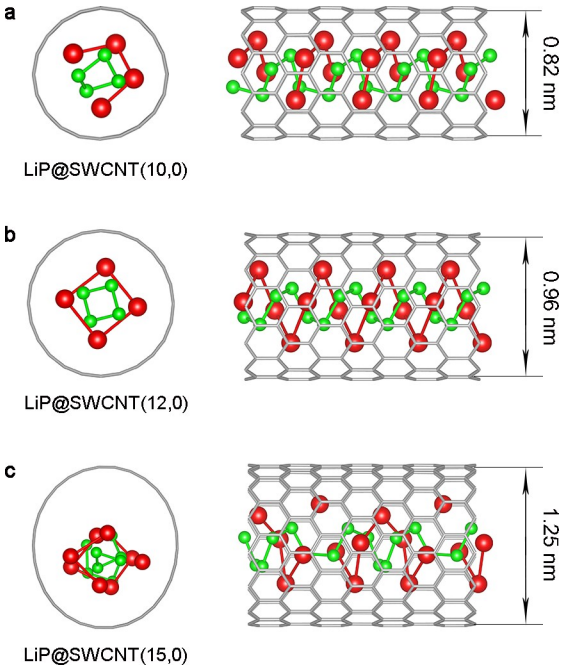

Fig. 2 End-on and side views of the fully optimized structures of LiP@SWCNT nanocomposites with the nanotube chiral indices of (a) (10,0), (b) (12,0), and (c) (15,0), respectively. Color scheme: Li, red; P, green; C, grey.

As can be seen from Fig. 2, for the thinnest SWCNT considered (SWCNT(10,0)), the large interaction between the SWCNT and LiP ionic chain slightly perturbs the double-helical motif. However, the SWCNT(12,0) was found to be the perfectly sized nanotube to accommodate the LiP double-helical nanowire. In this LiP@SWCNT(12,0) nanocomposite the balanced interaction between the nanotube and the LiP chain keeps both Li and P ions located right at the center of the SWCNT. With increasing diameter of nanotubes it is getting evident that positively charged Li cations are attracted to the SWCNT inner wall, dragging the whole LiP structure to the one of the nanotube directions. Consequently, the LiP adheres to the SWCNT wall, making

Nanoscale Accepted Manuscript

the (15,0) nanotube oval-shaped. The intercalation energies (per unit cell) were found to be 1.14, 0.35, and 2.07 eV for LiP@SWCNT(10,0), LiP@SWCNT(12,0), and LiP@SWCNT(15,0), respectively. It is interesting to note that the equilibrium structures of the LiP double helices confined within the SWCNTs are different from a free-standing LiP chain and those found in the bulk. According to our calculations, the pitch size of the nanotube encapsulated LiP chain decreased to 0.42 nm compared with the free-standing chain (0.48 nm) and P helices in the bulk $P2_1/c$ phase (0.49 nm). This phenomenon can be explained by the effect of the surrounding walls of nanotubes that compress the LiP double helices. While the P–P bond lengths in the LiP@SWCNT(12,0) decreased by ~0.08 Å, as compared to the free standing chain, the Li–P and Li–Li distances increased by ~0.5 Å and ~0.7 Å, respectively, due to the strong attraction of Li cations to the carbon nanotube,[51] which is consistent with the fact that C has a higher Pauling electronegativity value (2.55) than that of P atom (2.19). A full comparison of P–P, Li–P, and Li–Li bond lengths in the SWCNT(12,0) encapsulated LiP, free standing LiP, $P2_1/c$ phase LiP helices, and other experimentally obtained helical polyphosphides is given in Table S1 of the ESI†.

Geometry changes in the LiP structure indicate strong interaction with the corresponding SWCNTs that may give rise to a charge transfer. Therefore, to get more insight and demonstrate the effect of the charge transfer, we computed the electronic density redistribution for the LiP@SWCNT(10,0), LiP@SWCNT(12,0), and LiP@SWCNT(15,0) systems. In Fig. 3 we plotted the difference between the electronic density of the LiP@SWCNT nanocomposites and the sum of electronic densities of stand-alone LiP chains and the corresponding single-walled carbon nanotubes.

Nanoscale Accepted Manuscript

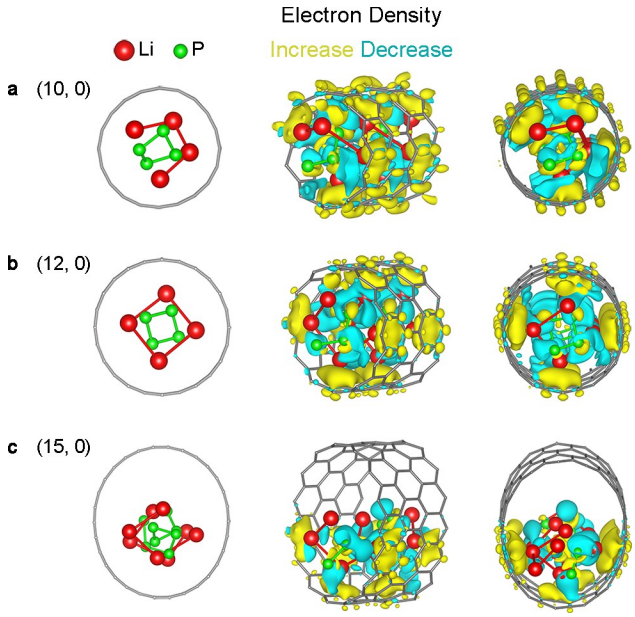

Fig. 3 Electronic density redistributions of the LiP ionic chains confined inside SWCNTs with chiral indices of (10,0), (12,0), and (15,0), respectively. Yellow and aqua blue colors denote an increase and decrease in electron charge density on intercalation as compared with the isolated systems. The isovalues are 15×10^{-4} a.u. for (a), 9×10^{-4} a.u. for (b), and 1×10^{-3} a.u. for (c).

For all systems considered, we observe the charge transfer, which results in net effective negative charge on the inner wall of the SWCNT and the increased positive charge on the P helical chain (Fig. 3). This creates an effective electric field inside the SWCNT, which, in turn, stabilizes the LiP 1D chain. To obtain a quantitative description of the observed picture, we evaluated the charge transfer using the Bader scheme.[52] The Bader analysis for a stand-alone LiP gave charges with magnitude of +0.84*e* on the Li and -0.84*e* on the P atoms, which is consistent with the ionic character of the LiP chain. Interestingly, the calculated charges for the LiP@SWCNT(12,0) system show Li atoms have the same charge of +0.84*e*, whereas the charge of P atoms drops to -0.62*e*. Therefore, the partial negative charge is transferred from the P helix to the inner wall of nanotube and the Li atoms just serve here as charge carrier particles. Indeed,

Nanoscale Accepted Manuscript

the Bader analysis confirms the partial negative charge on the C atoms in the LiP@SWCNT(12,0) system, ranging from -0.06*e* to -0.13*e*. Furthermore, the observed contraction of the P–P bonds in the encapsulated LiP structure can be explained by the decreasing repulsion between P anions due to the partial withdrawal of the electron density from the P helical strand.

The interaction between the LiP double-helix and the nanotube can also be clarified by an electronic structure analysis. Fig. 4 shows the calculated density of electronic states (DOS) of LiP@SWCNT(12,0), projected onto the constituent atomic orbitals. DOS for the stand-alone LiP and the SWCNT(12,0) are also shown for comparison. From Fig. 4 one can clearly see that the DOS of the SWCNT-encapsulated LiP double-helical nanowire is obviously broadened and up-shifted, with respect to their counterparts of the free standing LiP and SWCNT(12,0). This further confirms a strong interaction between the 1D LiP nanowire and the SWCNT, mainly due to the electrostatic interaction. Analysis of the electronic structures of LiP@SWCNT with different chiralities such as (10,0) and (15,0) (Fig. S1 and S2; Tables S2 and S3 of the ESI†) indicates a similar host–guest interaction, but the values of charge transfer from P helical chain to SWCNT vary slightly in different nanotubes. Since zigzag carbon nanotubes SWCNT(*n*,0) are generally expected to be metallic when *n* is a multiple of 3 (though Lieber er al.[53] experimentally showed that SWCNT(12,0) still has a small band gap of ~0.042 eV, which is in reasonable agreement with our band gap estimation (0.091 eV) for SWCNT(12,0)), it would be interesting to check whether inserting LiP inside a semiconducting nanotube is possible. Hence, we performed additional calculations for the LiP double helix confined into semiconducting SWCNT(13,0) with a diameter of 1.02 nm, which is only 0.07 nm larger than a diameter of "metallic" SWCNT(12,0). According to our results, the LiP double-helical motif remains

Nanoscale Accepted Manuscript

unperturbed inside SWCNT(13,0) and the DOS of the resulting LiP@SWCNT(13,0) nanocomposite is similar to that of LiP@SWCNT(12,0) (Fig. S3 of the ESI†).

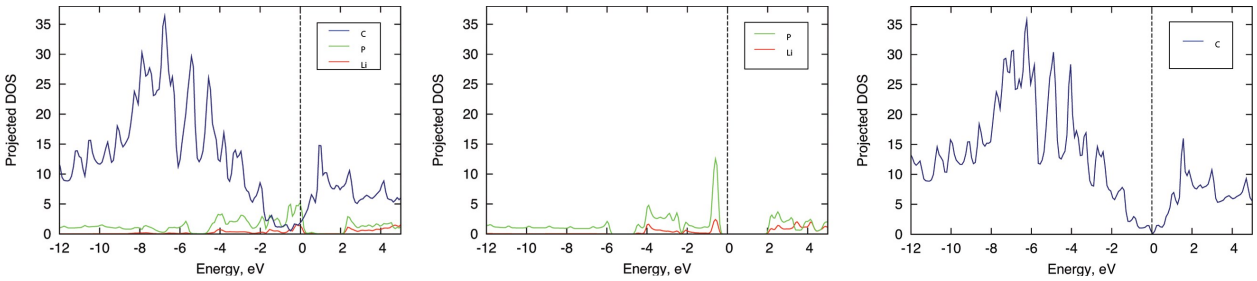

Fig. 4 Projected density of electronic states for the LiP@SWCNT(12,0) system (left), as well as for the stand-alone LiP double-helical chain (center) and the carbon nanotube (right).

In order to gain additional insight into the structure and chemical bonding in the SWCNT(12,0) encapsulated LiP double helix, we performed natural bond orbital (NBO)[54,55] and adaptive natural density partitioning (AdNDP)[56,57] analyses. NBO revealed one *s*-type and one *p*-type lone pair (LP) on each of the P atoms with an occupation number (ON) of 1.73 |e| and 1.82 |e|, respectively, and 2c-2e σ bonds (ON = 1.95 |e|) between P atoms in the phosphorus polyanion chain. The results of the AdNDP analysis are generally in agreement with the NBO results (Fig. 5). We also estimated the stabilization energy $E^{(2)}$ for LiP@SWCNT(12,0) using second-order perturbation theory, which is associated with electron delocalization between the donor and acceptor orbitals. The NBO analysis for LiP@SWCNT(12,0) system revealed some Li–P and Li–C interactions that play an important role in stabilizing the encapsulated double-helical LiP structure. The stabilization energy $E^{(2)}$ for $BD_{P\text{-}P} \rightarrow LP^*_{Li}$, $LP_P \rightarrow LP^*_{Li}$, and $BD_{C\text{-}C} \rightarrow LP^*_{Li}$ (where $BD_{P\text{-}P}$ denotes two-center P–P bond) interactions vary from 8.0 to 15.5 kcal mol^{-1}, 2.1 to 2.3 kcal mol^{-1}, and 5.1 to 13.0 kcal mol^{-1}, respectively. NBO analysis does not show any significant direct covalent bonding between Li atoms, thus the formation of helical Li strand is due to

Nanoscale Accepted Manuscript

favorable electrostatic interactions between lithium cations and neighboring phosphorus anions as well as carbon atoms of the SWCNT. However, the $E^{(2)}$ stabilization energies indicate significant interactions among the Li atoms. Several $LP^*_{Li} \rightarrow LP^*_{Li}$ and $CR_{Li} \rightarrow LP^*_{Li}$ (where CR_{Li} denotes a one-center Li core pair) interactions with $E^{(2)}$ ranging from 1.9 to 200.1 kcal mol^{-1} and from 1.2 to 3.7 kcal mol^{-1} are observed for the confined LiP chain. These results suggest that the empty (or partially filled) 2s orbitals of different Li atoms may significantly overlap. Such behavior of electropositive lithium atoms is typical for hyperlithiated species and was first noticed by Schleyer et al.,[58] who showed that the 12 pair-wise contacts between adjacent lithium atoms in CLi_6, contribute significant stabilization to the whole system. Overall, the noncovalent Li–P, Li–C, and Li–Li interactions significantly stabilize the double-helix framework of the SWCNT(12,0) encapsulated LiP nanowire.

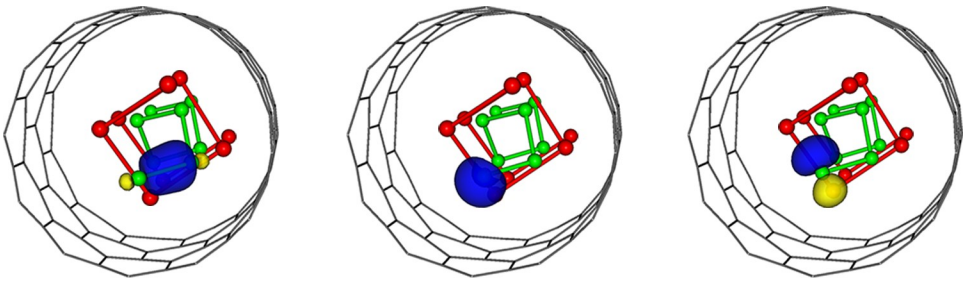

Fig. 5 AdNDP chemical bonding pattern for the LiP@SWCNT(12,0). The isovalue is 9×10^{-2} a.u.; ON stands for occupation numbers. All bonding elements are visualized for only one P atom in the unit cell. Li and P spheres were minimized for clarity.

Finally, to verify that this new nanomaterial will be stable at ambient conditions, we have performed constant-temperature (300 K) constant-volume *ab initio* molecular dynamics (MD) simulations of the LiP@SWCNT(12,0) system. Additional MD simulations were also carried out

Nanoscale Accepted Manuscript

to evaluate the thermal stability of the LiP@SWCNT(12,0) material at temperatures of 500 and 700 K. Fig. 5 shows snapshots taken at the end of each MD simulation and P–P bond lengths evolution in the encapsulated LiP nanowire for the last 2 ps.

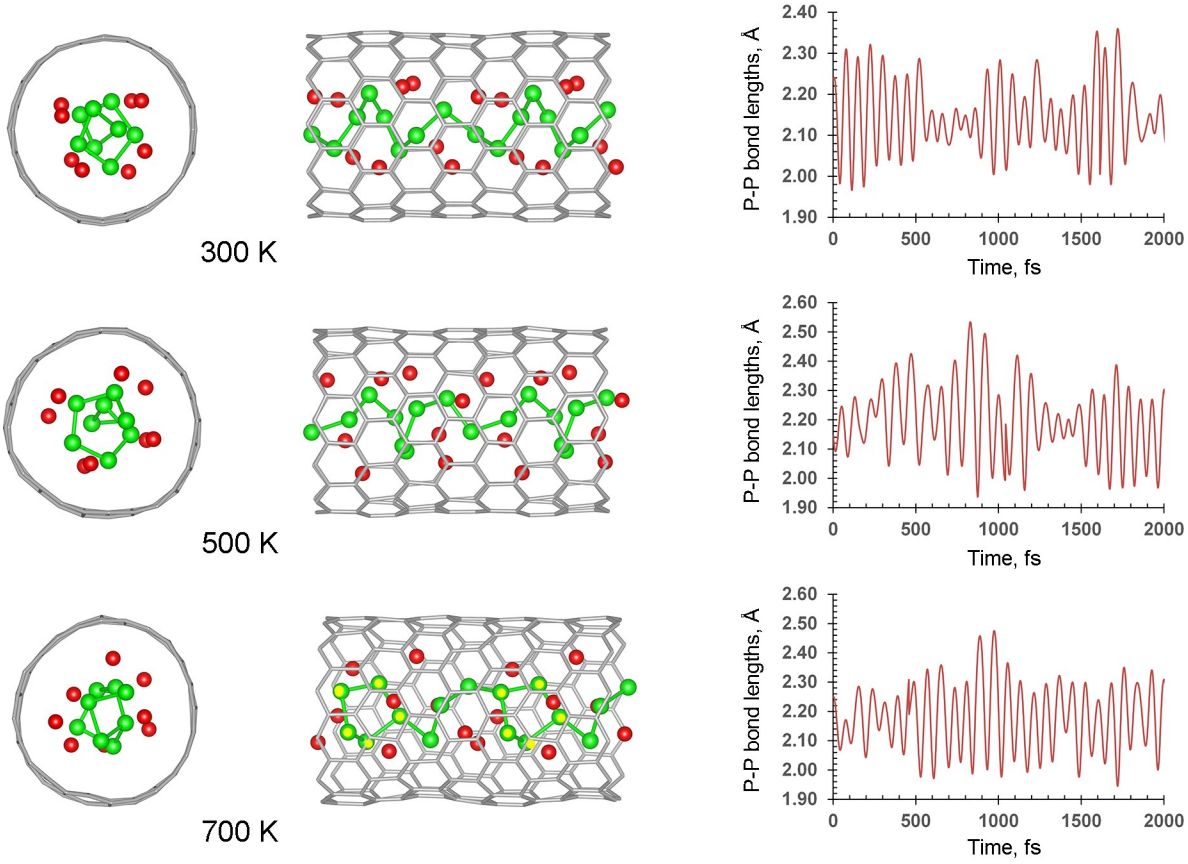

Fig. 6 Snapshots of the final frame of each MD simulation at 300, 500, and 700 K (end and side views), and the evolution of P–P bond lengths as temperature. Phosphorus atoms forming five-membered ring clusters (at 700 K) are highlighted in yellow. Color scheme: Li, red; P, green; C, grey.

As can be seen from Fig. 6, the double-helical motif of LiP remains stable and survives at 300 K. P–P bond lengths maximally increase by up to 16% at elevated temperature (500 K) in the last 2 ps of the simulation, but they stay shorter most of the time. At 700 K the P–P bond lengths also

Nanoscale Accepted Manuscript

oscillate in a reasonable range (2.0 – 2.6 Å), however, distances between the two adjacent P atoms of polyanion phosphorus helix are becoming too small leading to the formation of the five-membered ring clusters inside the nanotube. Therefore, the above results show that LiP@SWCNT(12,0) material has relatively good thermal stability and can maintain its double-helical morphology up to 500 K.

3. CONCLUSIONS

In conclusion, we have designed a new hybrid material, where the double-helical chain of lithium cations and phosphorus anions is encapsulated in carbon nanotubes. Based on our *ab initio* calculations, this material is stable and we observed the strong interaction between the LiP and CNTs that leads to a negative charge transfer from the polyphosphide helical chain to the walls of the CNTs. Considering the rapid development of experimental techniques and methods for encapsulation of 1D crystals in recent years, there is a hope that the predicted nanomaterial will be produced in the near future. Although there were earlier reports on inorganic double-helix structures of nanotube confined Se[48] and I,[49] if the inorganic LiP is confirmed experimentally, it would be the first example of 1D inorganic double-helix comprising both anions and cations. We also believe that the presented confinement in nanotubes may become a new approach applicable for the synthesis of a plethora of other one-dimensional Zintl polyphosphide chains,[59-61] which possess unique structural features and exceptional properties suitable for applications in the fields of Li- and Na-ion batteries, catalysis, and thermoelectrics.

4. METHODS

First-principles calculations were carried out using VASP - the Vienna ab initio simulation package.[62-64] The Kohn–Sham equations were solved using the projector-augmented wave

Nanoscale Accepted Manuscript

(PAW) method.[65,66] Standard PAW potentials were employed for the elemental constituents, with valence configurations of $2s^1 2p^0$ for Li, $3s^2 3p^3$ for P, and $2s^2 2p^2$ for C. The exchange and correlation interactions are described by the Perdew–Burke–Ernzerhof (PBE) functional.[67,68] The Brillouin-zone integrations were performed on a dense Γ-centered 1 × 1 × 7 k-point grid initially for a small unit cell, i.e. [LiP@SWCNT(12,0): 4 Li, 4 P, and 48 C atoms], and 1 × 1 × 3 k-point grid for a larger unit cell, i.e. [LiP@SWCNT(12,0): 8 Li, 8 P, and 96 C atoms].[69] The kinetic energy cutoff for plane waves was set to 600 eV and the "high" precision setting was chosen to avoid wrap around errors. The criteria for convergence in energy and force was set to 10^{-6} eV and 0.001 eV/Å, respectively. A vacuum space of approximately 20 Å was introduced to ensure the periodic images are well separated. The intercalation energy (ΔE) between the stand-alone LiP chain and the corresponding SWCNT was defined as ΔE = E(LiP) + E(SWCNT) – E(LiP@SWCNT). The charge transfer in the studied systems has been evaluated using the Bader scheme.[52]

To assess the thermal stability of the LiP@SWCNT(12,0) composite, *ab initio* molecular dynamics (MD) simulations were performed using VASP and employing the PAW potentials and the PBE functional given above. Simulations using an NVT ensemble at 300, 500, and 700 K with a time step of 1 fs were carried out for 10 ps. The kinetic energy cutoff for plane waves in these calculations was reduced to the default with the "normal" precision setting specified.

Chemical bonding analysis of the LiP@SWCNT(12,0) was performed on a LiP@SWCNT(12,0) fragment extracted from the periodic structure and capped with hydrogen atoms at the PBE1PBE/6-31G(d) level of theory[67,68,70] (Gaussian 09 simulation package)[71] using the adaptive natural density partitioning (AdNDP) method.[56,57] AdNDP is an extension of the natural bonding orbital (NBO) method[54,55] and analyzes the first-order reduced density matrix in order to obtain

Nanoscale Accepted Manuscript

its local block eigenfunctions with optimal convergence properties for an electron density description. The obtained local blocks correspond to the sets of n atoms (n ranging from one to the total number of atoms in the molecule) that are tested for the presence of two-electron objects (n-center two electron (nc-2e) bonds, including core electrons and lone pairs as a special case of n = 1) associated with this particular set of n atoms. AdNDP accepts only those bonding elements whose occupation numbers (ONs) exceed the specified threshold values, which are usually chosen to be close to 2.00 |e|. The Visualization for Electronic and Structural Analysis software (VESTA, series 3)[72] was used for structure visualization.

ASSOCIATED CONTENT

†Electronic supplementary information (ESI) available: additional DOS, band structures, and Bader charges for LiP@SWCNTs. See DOI: 10.1039/x0xx00000x

ACKNOWLEDGMENTS

This work was supported by the National Science Foundation (CHE-1361413 to A.I.B.). Computer, storage and other resources from the Division of Research Computing in the Office of Research and Graduate Studies at Utah State University and the Center for High Performance Computing at the University of Utah are gratefully acknowledged.

REFERENCES

1) R. Zan, Q. M. Ramasse, U. Bangert and K. S. Novoselov, *Nano Lett*., 2012, **12**, 3936–3940.

Nanoscale Accepted Manuscript

2) A. Neto, F. Guinea, N. Peres, K. Novoselov and A. Geim, *Rev. Mod. Phys.*, 2009, **81**, 109–162.

3) Q. H. Wang, K. Kalantar-Zadeh, A. Kis, J. N. Coleman and M. S. Strano, *Nature Nanotech.*, 2012, **7**, 699–712.

4) B. Radisavljevic, A. Radenovic, J. Brivio, V. Giacometti and A. Kis, *Nature Nanotech.*, 2011, **6**, 147–150.

5) H. O. H. Churchill and P. Jarillo-Herrero, *Nature Nanotech.*, 2014, **9**, 330–331.

6) H. Liu, A. T. Neal, Z. Zhu, Z. Luo, X. Xu, D. Tomanek and P. D. Ye, *ACS Nano*, 2014, **8**, 4033–4041.

7) S. Bartha, F. Hernandez-Ramirezc, J. D. Holmesa and A. Romano-Rodriguez, *Progress in Mater. Sci.*, 2010, **55**, 563–627.

8) A. M. Morales and C. M. Lieber, *Science*, 1998, **279**, 208–211.

9) J. D. Holmes, K. P. Johnson, R. C. Doty and B. A. Korgel, *Science*, 2000, **287**, 1471–1473.

10) T. J. Trentler, K. M. Hickman, S. C. Goel, A. M. Viano, P. C. Gibbons and W. E. Buhro, *Science*, 1995, **270**, 1791–1794.

11) M. S. Gudiksen, L. J. Lauhon, J. Wang, D. C. Smith and C. M. Lieber, *Nature*, 2002, **415**, 617–620.

12) Z. W. Pan, Z. R. Dai and Z. L. Wang, *Science*, 2001, **291**, 1947–1949.

Nanoscale Accepted Manuscript

13) H. F. Zhang, A. C. Dohnalkova, C. M. Wang, J. S. Young, E. C. Buck and L. S. Wang, *Nano Lett*., 2002, **2**, 105.

14) Z. L. Wang, *Adv. Mater*., 2003, **15**, 432–436.

15) Y. Zhang, K. Suenaga, C. Colliex and S. Iijima, *Science*, 1998, **281**, 973–975.

16) G. Zhang, H. B. Wu, H. E. Hostera and X. W. Lou, *Energy Environ. Sci*., 2014, **7**, 302–305.

17) Y. Kondo and K. Takayanagi, *Science*, 2000, **289**, 606–608.

18) J. Bettini, F. Sato, P. Z. Coura, S. O. Dantas, D. S. Galvão and D. Ugarte, *Nature Nanotech*., 2006, **1**, 182–185.

19) B. Hong, S. Bae, C. Lee, S. Jeong and K. Kim, *Science*, 2001, **294**, 348–351.

20) I. M. Mikhailovskij, N. Wanderka, V. A. Ksenofontov, T. I. Mazilova, E. V. Sadanov and O. A. Velicodnaja, *Nanotechnology*, 2007, **18**, 475705.

21) C. Jin, H. Lan, L. Peng, K. Suenaga and S. Iijima, *Phys. Rev. Lett*., 2009, **102**, 205501.

22) A. Chuvilin, J. C. Meyer, G. Algara-Siller and U. Kaiser, *New J. Phys*., 2009, **11**, 083019.

23) H.-F. Zhang, C.-M. Wang and L.-S. Wang, *Nano Lett*., 2002, **2**, 941–944.

24) C. C. Easterday, L. R. Dedon, M. Zeller and C. M. Oertel, *Cryst. Growth Des*., 2014, **14**, 2048–2055.

Nanoscale Accepted Manuscript

25) S. Meister, H. Peng, K. McIlwrath, K. Jarausch, X. F. Zhang and Y. Cui, *Nano Lett.,* 2006, **6**, 1514–1517.

26) M. Yanga and N. A. Kotov, *J. Mater. Chem.*, 2011, **21**, 6775–6792.

27) J. K. Hirschberg, L. Brunsveld, A. Ramzi, J. M. Vekemans, R. P. Sijbesma and E. W. Meijer, *Nature*, 2000, **407**, 167–170.

28) V. Berl, I. Huc, R. G. Khoury, M. J. Krische and J. M. Lehn, *Nature*, 2000, **407**, 720–723.

29) J. D. Watson and F. H. C. Crick, *Nature*, 1953, **171**, 737–738.

30) D. Rhodes and A. Klug, *Nature*, 1980, **286**, 573–578.

31) M.-Q. Zhao, Q. Zhang, G.-L. Tiana and F. Wei, *Nanoscale*, 2014, **6**, 9339–9354.

32) H. Morito and H. Yamane, *Angew. Chem. Int. Ed.*, 2010, **49**, 3638–3641.

33) E. D. Sone, E. R. Zubarev and S. I. Stupp, *Small*, 2005, **1**, 694–697.

34) Q. Zhang, M.-Q. Zhao, D.-M. Tang, F. Li, J.-Q. Huang, B. Liu, W.-C. Zhu, Y.-H. Zhang and F. Wei, *Angew. Chem., Int. Ed.*, 2010, **49**, 3642–3645.

35) Y. Wang, Q. Wang, H. Sun, W. Zhang, G. Chen, Y. Wang, X. Shen, Y. Han, X. Lu and H. Chen, *J. Am. Chem. Soc.*, 2011, **133**, 20060–20063.

36) A. S. Ivanov, A. J. Morris, K. V. Bozhenko, C. J. Pickard and A. I. Boldyrev, *Angew. Chem., Int. Ed.,* 2012, **51**, 8330–8333.

Nanoscale Accepted Manuscript

37) A. K. Jissy and A. Datta, *J. Phys. Chem. Lett.*, 2013, **4**, 1018–1022.

38) J. Hentschel, A. M. Kushner, J. Ziller and Z. Guan, *Angew. Chem., Int. Ed.*, 2012, **51**, 10561–10565.

39) Y. Amamoto, J. Kamada, H. Otsuka, A. Takahara and K. Matyjaszewski, *Angew. Chem., Int. Ed.*, 2011, **50**, 1660–1663.

40) J. Sloan and M. Monthioux, *Filled carbon nanotubes (X@CNTs) Carbon Meta-Nanotubes: Synthesis, Properties and Applications (ed. by M. Monthioux)*, 2012, 225–271. John Wiley & Sons Ltd., Chichester, UK.

41) J. Sloan, A. I. Kirkland, J. L. Hutchison and M. L. H. Green, *Chem. Commun.*, 2002**,** **2002**, 1319–1332.

42) J. Sloan, A. I. Kirkland, J. L. Hutchison and M. L. H. Green, *C. R. Phys.*, 2003, **4**, 1063–1074.

43) R. Senga, H. P. Komsa, Z. Liu, K. Hirose-Takai, A. V. Krasheninnikov and K. Suenaga, *Nature Mat.*, 2014, **13**, 1050–1054.

44) T. Fujimori, A. Morelos-Gómez, Z. Zhu, H. Muramatsu, R. Futamura, K. Urita, M. Terrones, T. Hayashi, M. Endo, S. Y. Hong, Y. C. Choi, D. Tománek and K. Kaneko, *Nature Commun.*, 2013, **4**, 2162–2169.

45) H. W. Ch. Postma, T. Teepen, Z. Yao, M. Grifoni and C. Dekker, *Science*, 2001, **293**, 76–79.

Nanoscale Accepted Manuscript

46) A. Bachtold, P. Hadley, T. Nakanishi and C. Dekker, *Science*, 2001, **294**, 1317–1320.

47) T. Rueckes, K. Kim, E. Joselevich, G. Y. Tseng, C.-L. Cheung and C. M. Lieber, *Science*, 2000, **289**, 94–97.

48) T. Fujimori, R. B. dos Santos, T. Hayashi, M. Endo, K. Kaneko and D. Tomanek, *ACS Nano*, 2013, **7**, 5607–5613.

49) X. Fan, E. C. Dickey, P. C. Eklund, K. A. Williams, L. Grigorian, R. Buczko, S. T. Pantelides and S. J. Pennycook, *Phys. Rev. Lett.*, 2000, **84**, 4621–4624.

50) W. Hönle and H.-G. Z. von Schnering, *Kristallogr.*, 1981, **155**, 307–314.

51) T. Kar, J. Pattanayak and S. Scheiner, *J. Phys. Chem. A,* 2001, **105**, 10397–10403.

52) W. Tang, E. Sanville and G. A. Henkelman, *J. Phys.: Condens. Matter.*, 2009, **21**, 084204.

53) M. Ouyang, J.-H. Huang, C. L. Cheung, C. M. Lieber, *Science*, 2001, **292**, 702–705.

54) J. P. Foster and F. Weinhold, *J. Am. Chem. Soc.*, 1980, **102**, 7211–7218.

55) F. Weinhold and C. R. Landis, *Valency and Bonding, a Natural Bond Orbital Donor–Acceptor Perspective; Cambridge University Press: Cambridge*, 2005.

56) D. Y. Zubarev and A. I. Boldyrev, *Phys. Chem. Chem. Phys.*, 2008, **10**, 5207–5217.

57) T. R. Galeev, B. D. Dunnington, J. R. Schmidt and A. I. Boldyrev, *Phys. Chem. Chem. Phys.*, 2013, **15**, 5022–5029.

Nanoscale Accepted Manuscript

58) P. v. R. Schleyer, E. U. Wiirthwein, E. Kaufmann, T. Clark, J. A. Pople, *J. Am. Chem. Soc.*, 1983, **105**, 5930-5932.

59) H. G. von Schnering and W. Hoenle, *Chem. Rev.*, 1988, **88**, 243–273.

60) J. Fulmer, D. Kaseman, J. Dolyniuk, K. Lee, S. Sen and K. Kovnir, *Inorg. Chem.*, 2013, **52**, 7061–7067.

61) J.-A. Dolyniuk, H. He, A. S. Ivanov, A. I. Boldyrev, S. Bobev and K. Kovnir, *Inorg. Chem.*, 2015, **54**, 8608–8616.

62) G. Kresse and J. Furthmüller, *Comput. Mater. Sci.*, 1996, **6**, 15–50.

63) G. Kresse and J. Furthmüller, *Phys. Rev. B,* 1996, **54**, 11169–11186.

64) G. Kresse and J. Hafner, *Phys. Rev. B,* 1993, **47**, 558–561.

65) P. E. Blöchl, *Phys. Rev. B,* 1994, **50**, 17953–17979.

66) G. Kresse and D. Joubert, *Phys. Rev. B,* 1999, **59**, 1758–1775.

67) J. P. Perdew, K. Burke and M. Ernzerhof, *Phys. Rev. Lett.*, 1996, **77**, 3865–3868.

68) J. P. Perdew, K. Burke and M. Ernzerhof, *Phys. Rev. Lett.*, 1997, **78**, 1396–1396.

69) H. J. Monkhorst and J. D. Pack, *Phys. Rev. B,* 1976, **13**, 5188–5192.

70) G. A. Petersson and M. A. Al-Laham, *J. Chem. Phys.*, 1991, **94**, 6081–6090.

Nanoscale Accepted Manuscript

71) M. J. Frisch, G. W. Trucks, H. B. Schlegel, G. E. Scuseria, M. A. Robb, J. R. Cheeseman, G. Scalmani, V. Barone, B. Mennucci and G. A. Petersson, *Gaussian 09, revision B.01; Gaussian, Inc.: Wallingford, CT*, 2009.

72) K. Momma and F. Izumi, *J. Appl. Crystallogr.*, 2011, **44**, 1272–1276.

We demonstrate a prediction of a novel hybrid material, nanotube encapsulated 1D ionic LiP double-helix structure, suggesting that nanostructured confinement may be used to stabilize other Zintl polyphosphide chains.

Table of Contents

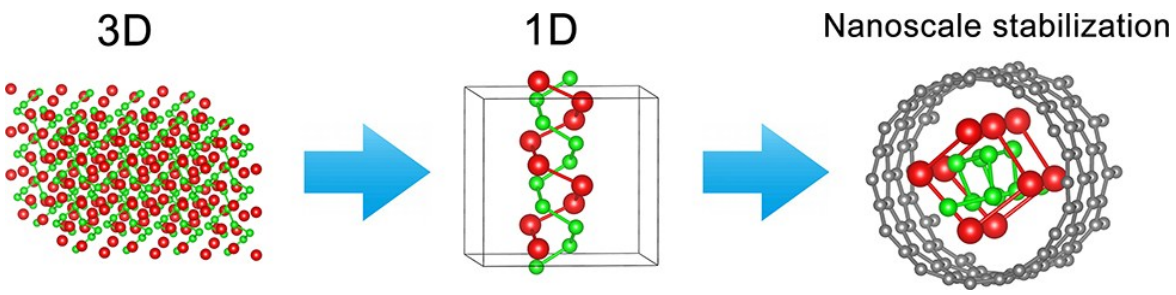

Nanoscale Accepted Manuscript